Analysis of a Concept Focusing Lens for SSR0 Section of PX Linac

I. Terechkine

I. Introduction

As it was shown in [1] and [2], solenoid-based focusing lenses have spherical aberrations that can result in beam emittance increase. Study in [1] was conducted for the lenses built for use in the CH and SS1 sections of the HINS linac front end [3] and for a concept lens (SS0) for the initial section of the proposed front end of the PX linac [4]. In all cases, the study used a beam which was initially parallel to the geometric axis of the lenses. For the SS0 concept lens, it was shown that if the beam radius exceeded ~7.5 mm inside the lens, one can expect some growth of the emittance. Besides the issue of the emittance growth, we need to understand to which extent uncertainties in the lens alignment and construction can result in deterioration of the lens optical properties. To set the initial point of this study, concept SS0 lens model used in [1] will be used again with the maximum beam radius of 8 mm and the initial normalized emittance of 0.4 π mm·mrad. Then the next manipulations with the lens will be made to see what impact on the emittance each particular action has:

1. The lens will be shifted by 1 mm and 2 mm;
2. The lens will be tilted around the center point by 5 mrad;
3. One of the bucking coils of the lens will be shifted by 0.5 mm and 1 mm.

In all the cases, the input plane is at X = -200 mm, and the output plane coincides with the rear focal plane of the lens.

Before we start charged particle tracking, let's understand what emittance growth is expected if thin, optical-type (focus both in Y and Z directions, and no image rotation occurs) lenses are used for beam transport. Spherical aberrations in the lenses are similar to those in the concept SS0 lens. Focusing length of a solenoid-based lens is defined by the expression

$$f = \frac{8 \cdot \frac{m}{q} \cdot U}{\int_{-\infty}^{+\infty} B_X^2 dX}$$

where U is energy of charged particles in eV (mass m [kg] and charge q [C]) and B_X is longitudinal magnetic field in Tesla. The expression in the denominator defines the lens strength (integrated strength) and is chosen ~1.8 T^2·m, which implies the current in the lens of ~185 A. This strength of the lens and the sample particle energy of 2.5 MeV were chosen to make the model more compact to reduce required memory. The distance from the center of the lens to the focal point for particles traveling close to the axis is ~128.7 mm for 2.5 MeV proton beam; we will call this distance focal length in further discussion.

According to [1] (see Table 2 in [1]), the integrated strength increases with radius. Hence, focusing length becomes smaller, which translates into typical spherical aberration, when the focal length of the lens is dependent on the distance r from the axis; this dependence can be expressed in the form $f(r) = f0 \cdot (1 - r^2/R0^2)$, where R0 is a parameter that defines the scale of

the aberration. In the case of the concept SS0 lens in [1], R0 = 56.7 mm. Dependence of the focal length on the distance *r* for the concept lens is shown in Fig. 1.

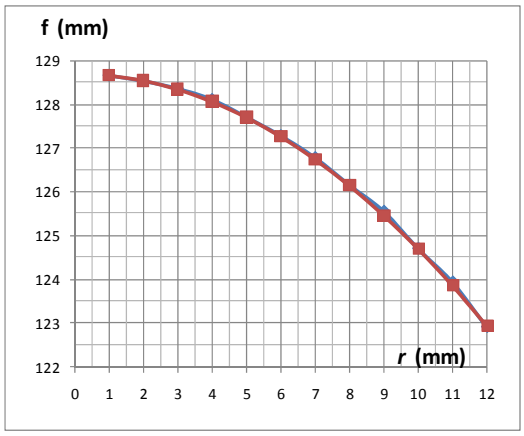

Fig. 1. Focal length as a function of the radial distance for the SS0 concept lens

Fig. 2 shows effective emittance diagram for an 8-mm radius beam in the vicinity of a rear focal plane of an optical lens with the focal length (*f0* = 128.7 mm); the beam is parallel before entering the lens.

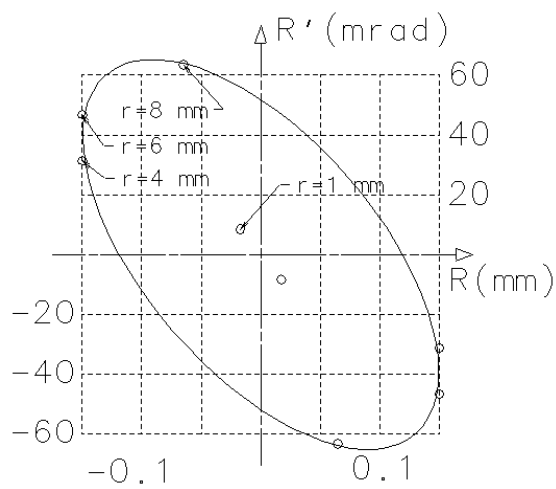

Fig. 2. Effective emittance increase due to spherical aberration for an optical lens

As it is clear from the diagram in Fig. 2, one can expect significant growth of the emittance if r > 6 mm. Case with r = 10 mm results in about three-fold increase of the emittance.

Normalized emittance corresponding to the ellipse in Fig. 2 is ~0.5 π mm-mrad; it must be compared with the desired normalized emittance of the beam of ~0.25 π mm-mrad. Because we used radius as an argument in the emittance diagram, transition to the transverse coordinates Y or Z will result in twice as low emittance. Nevertheless, this emittance growth is still high, and we need to further study the issue to be sure the lens can be used for beam transport. Particularly, effect of beam rotation must be taken into account.

II. Witness run: no shift, no tilt

Using a 3D electromagnetic model of the concept lens allows us to investigate the issue without making any special assumptions or linearization. First, we will use "perfect" SS0 lens without any shift or tilt. The input system of the sample traces is designed so that the area they occupy on the phase plane is 0.4 π mm-mrad after normalization (β = 0.0729). The initial conditions for the sample traces are summarized in Table 1.

Table 1

	Y0 (mm)	Y0' (mrad)	Z0 (mm)	Z0" (mrad)
1	8	0	0	0
2	5.66	5.66	0	0
3	0	8	0	0
4	-5.66	5.66	0	0
5	-8	0	0	0
6	-5.66	-5.66	0	0
7	0	-8	0	0
8	5.66	-5.66	-0	0
9	8	0	0	0.686
10	8	0	0	-0.686
11	-8	0	0	0.686
12	-8	0	0	-0.686
13	0	8	0.686	0
14	0	8	-0.686	0
15	0	-8	0.686	0
16	0	-8	-0.686	0

Phase coordinates of each trace are analyzed in the vicinity of the rear focal plane. Snapshot of the emittance (X = 126 mm) is shown in Fig. 3. Two graphs in the diagram reflect phase coordinates of sample traces in the Y-Y' and Z-Z' planes. The circles in the figure represent the sample traces with zero transverse velocities, and the triangles correspond to the traces with

the transverse velocities of ~15000 m/s (or the initial trajectory angle 0.686 mrad). The area of the representing ellipse in Fig. 3 (both for the Y-Y' and Z-Z' plane) corresponds to the normalized emittance of ~0.42 π mm·rad. This value of the emittance is in agreement with the study in [1] for R_{max} = 7.5 mm. Some deviations from the initial emittance (or uncertainty of the emittance calculation) are inevitable due to a way the representing ellipse is chosen; as it was obvious in [1], significant growth of the emittance strongly manifests itself. As expected (due to the axial symmetry), the phase diagrams for the X-X' and Z-Z' planes are identical. They also symmetrical relative to the axes; because the emiitance is sampled near the focus plane, the coordinates in the graphs are small, while the angles are relatively large.

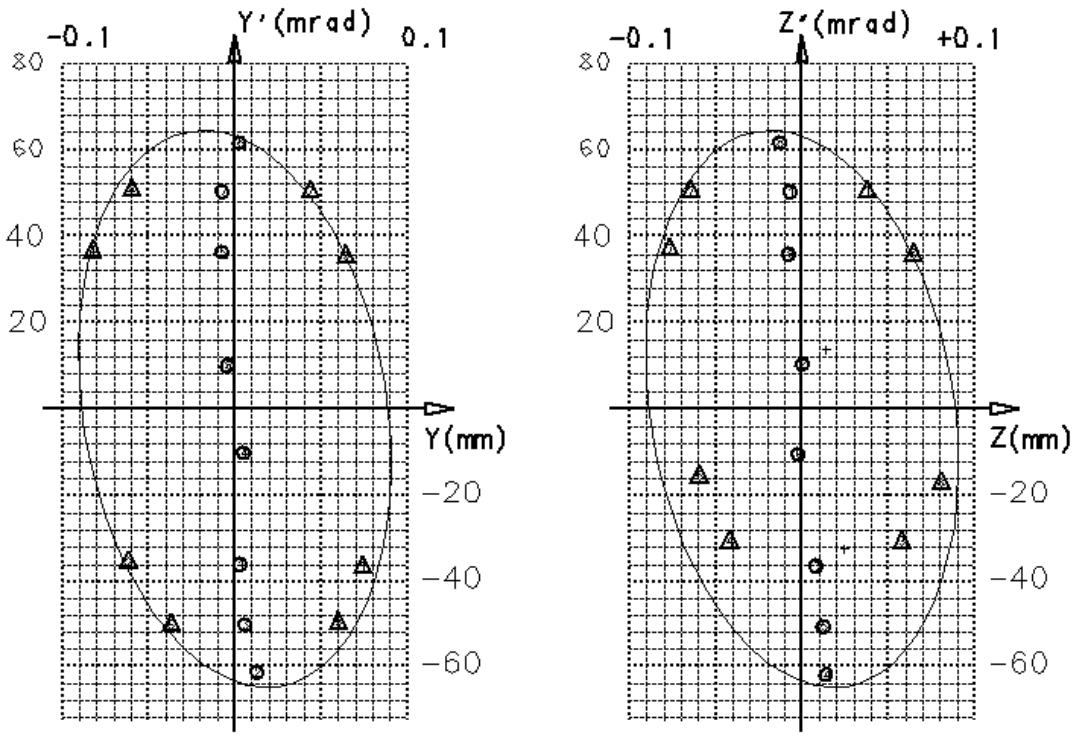

Fig. 3. Emittance diagram of the beam in the rear focal plane of the focusing lens; R_{max} = 8 mm, no shift, no tilt.

Emittance growth in the lens is significantly smaller than could be expected based on our first evaluation summarized in Fig. 1. Most probably, this important difference is due to rotation of the beam cross-section, that brings all peripheral trajectories closer to the axis.

The next step will be to apply certain defects to the lens positioning and assembly to understand their impact on the beam quality.

III. The lens is shifted in the transverse direction

During this study, adjustment of the lens position relative to the beam axis by parallel shift was made to allow direct comparison of the results with the ideal case (Fig. 3). Corresponding current density transformation in the lens model was made to reflect the shift. The same initial

conditions table (Table 1) was used for this run. Emittance diagrams in Fig. 4 reflect the case with the shift ΔZ = 1 mm and were taken in the plane Z = 126 mm (as before). Similar diagrams for the case ΔZ = 2 mm are shown in Fig. 5. In both cases, as it was possible to predict, the phase space diagram is shifted both in the direction of the coordinates and in the direction of the velocities. Calculating area within the representing ellipse, we can find the normalized emittances both in the Y-Y' and in Z-Z' planes : $\varepsilon_n \approx 0.52$ π·mm·rad for the case ΔZ = 1 mm and $\varepsilon_n \approx 0.64$ π·mm·rad for the case ΔZ = 2 mm. Growth rate of the emittance is close to linear, so with ΔZ = 0.3 mm, which is allowed limit of the lens displacement, we can expect ~10% emittance growth, which seems acceptable. Modeling of the beam propagation in the Front End of the PX accelerator front end implies much smaller beam size, so we could expect quite modest emittance growth due to this imperfectness.

At the exit of the lens, the beam, which was initially parallel to the lens axis, has transverse component of the velocity resulting in the angle $\varphi = \Delta Z/f$ = 1/126 ≈ 8 mrad for ΔZ = 1 mm. This angle must be compensated to avoid even larger offset at the location of the next lens. The dipole field integral required for this compensation is $BL = \varphi \cdot \beta c \cdot m/e$. For φ = 8 mrad, this results in BL ≈ 0.18 T-cm. To avoid significant increase of the offset at the position of the next lens (at 60 cm between the lenses, the offset can reach ~5 mm), it is desirable to make this compensation at the location of the shifted lens.

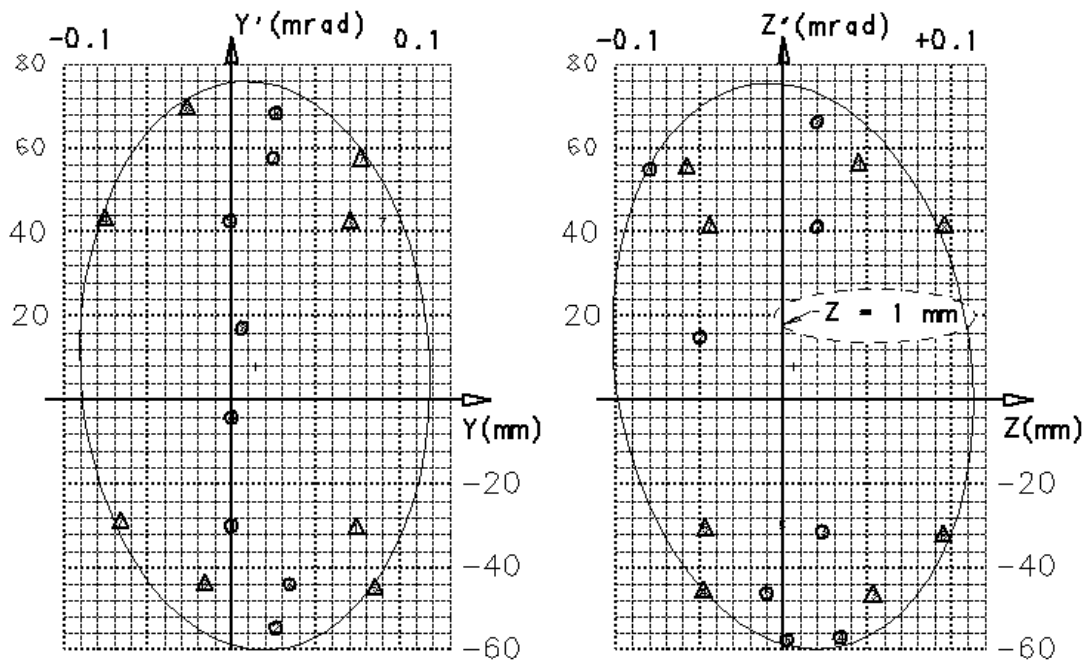

Fig. 4. Emittance diagram of the beam in the rear focal plane of the focusing lens; R_{max} = 8 mm, shift 1 mm, no tilt.

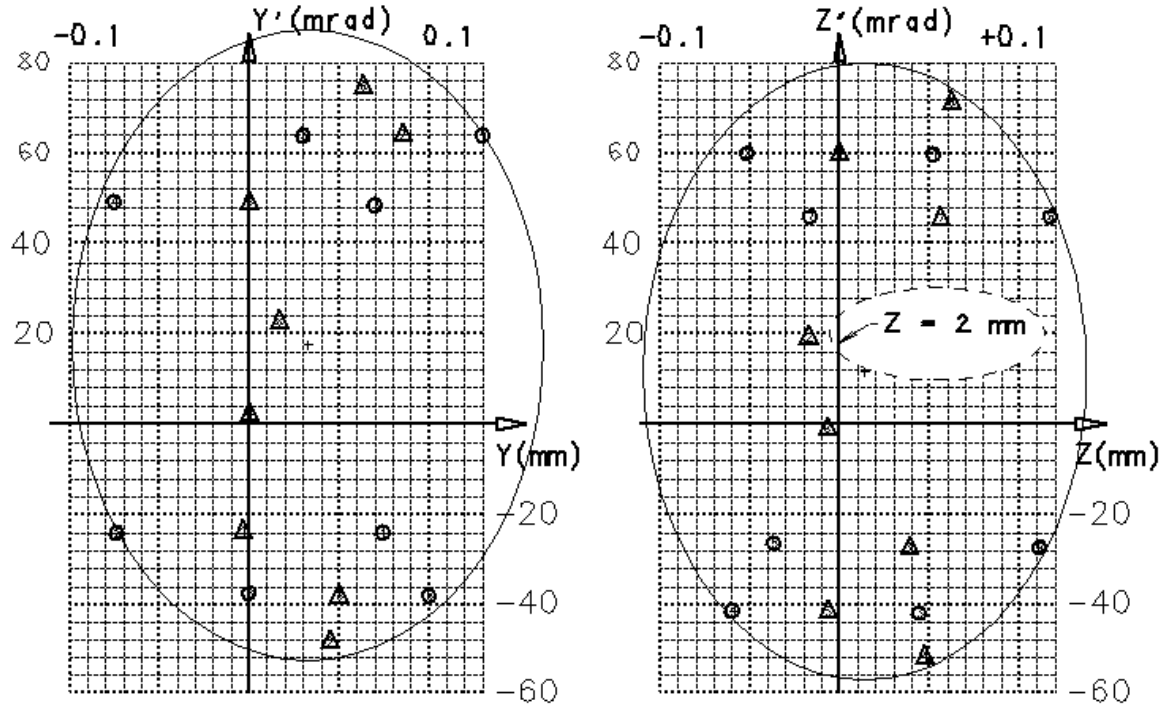

Fig. 5. Emittance diagram of the beam in the rear focal plane of the focusing lens; R_{max} = 8 mm, shift 2 mm, no tilt.

IV. Lens is tilted

As was done for the shifted lens case, we will adjust the position of the lens relative to the beam axis to allow direct comparison of the results with the ideal case (Fig. 3). The lens will be rotated around the Y axis, that passes through the center of the main coil. When this transformation is made, the current density in the coils will have not only Y and Z components, but also the X component. Sketch in Fig. 6 below helps to calculate all the components of the current density.

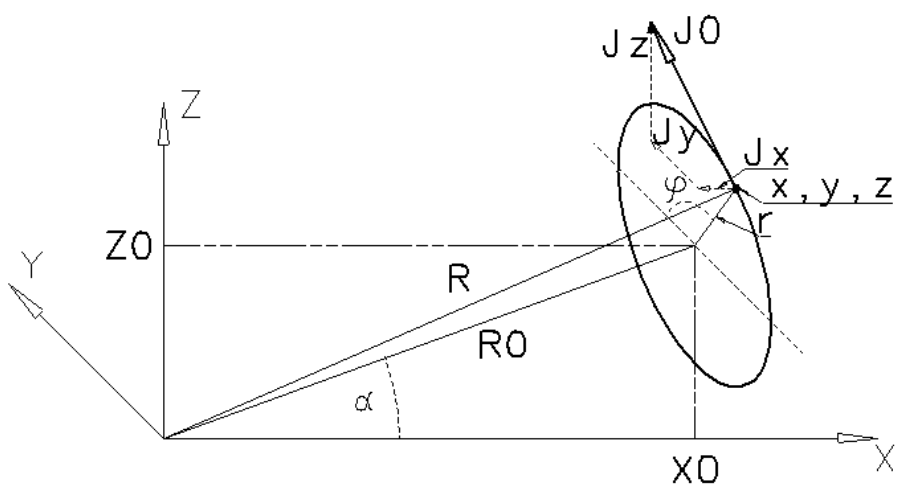

Fig. 6. Calculating current density vector components in the tilted coil.

The angle α defines the solenoid tilt angle. Because the solenoid axis is in the XZ plane, we can find coordinates of a center of any current loop:

$$X0 = R0\cdot\cos(\alpha),\ Z0 = R0\cdot\sin(\alpha) \qquad /1/$$

where R0 is the distance from the center of the lens to the plain of the current loop.
At any point inside the coil, the current loop radius can be found as

$$r^2 = (x-X0)^2 + y^2 + (z-Z0)^2 \qquad /2/$$

Distance R0 can be calculated as

$$R0^2 = R^2 - r^2 \qquad /3/$$

where R is a distance from the center of the solenoid to any point (x,y,z) on the current loop:

$$R^2 = x^2 + y^2 + z^2 \qquad /4/$$

Solving the equation system /1/ to /4/, we get

$$R0 = x\cdot\cos(\alpha) + z\cdot\sin(\alpha) \qquad /5/$$

and

$$r^2 = [x\cdot\sin(\alpha) - z\cdot\cos(\alpha)]^2 + y^2 \qquad /6/$$

Knowing r, it is possible to find position of the point of interest in the current loop relative to the Y direction:

$$\cos(\varphi) = y/r \qquad /7/$$

Finally, the components of the current density in the coil can be written as

$$Jy = J0\cdot\sin(\varphi) = J0\cdot\mathrm{sqrt}[1-(y/r)^2], \qquad /8/$$

where the sign of the current density J0 is positive if it is pointed towards increasing angle φ,

$$Jx = J0\cdot\cos(\varphi)\cdot\sin(\alpha) \qquad /9/$$

and

$$Jz = -J0\cdot\cos(\varphi)\cdot\cos(\alpha) \qquad /10/$$

Naturally, $Jx^2 + Jy^2 + Jz^2 = J0^2$.

Let's make α = 5 mrad (0.28648°). This tilt angle results in the distance of 1 mm between the geometric axis of the solenoid and the beam at 200 mm from the solenoid center. At the distance of one halve of the effective length (~100 mm), this deflection is ~0.25 mm, that is of the order of the required accuracy of the HINS solenoid alignment. Corresponding emittance diagrams in Fig. 7 must be compared with those in Fig. 3.

First thing to notice is that the beam centroid in the rear focal plane Z = 126 mm is shifted both in Y (by ~0.525 mm) and in Z (by ~0.255 mm), which is due to the deflecting by the Z component of the longitudinal magnetic field of the tilted lens and rotating by the X-component of the field. The beam comes out of the lens tilted in Y and Z planes (~ 4 mrad in both planes). Emittance of the beam does not change much though: both in Y and in Z planes, it is ~0.42 π mm-mrad. This is probably because the beam, while in the lens, is never too far from the lens axis, so the spherical aberration does not have a chance to manifest itself. If not to take correction measures, the displacement of the beam at the location of the next lens (600 mm distance) in the transport channel would be ~3.6 mm. This will result in significant aberration and emittance growth, as we saw in the previous chapter. So, proper alignment requirements must be set and compensation of possible tilt in each focusing element must be planned for. E.g. if to allow 5 mrad tilt, correctors must be able to compensate the transverse component of

the longitudinal magnetic field, which is ~300 Gs. This transverse component provides a kick of ~0.3 T-cm. Requirements for dipole corrector strength in the CH-type lenses are 0.25 T-cm, so allowed tilt based on this requirement cannot be more than ~4 mrad, which translates in ~0.4 mm positioning accuracy at the location of the alignment fiducials and compares well with the existing requirements for the lens positioning of ~0.3 mm. Correctors developed for the SS1 lens [5] of HINS can provide a kick of ~0.5 T-cm at 30 A, so even larger tilt can be tolerated.

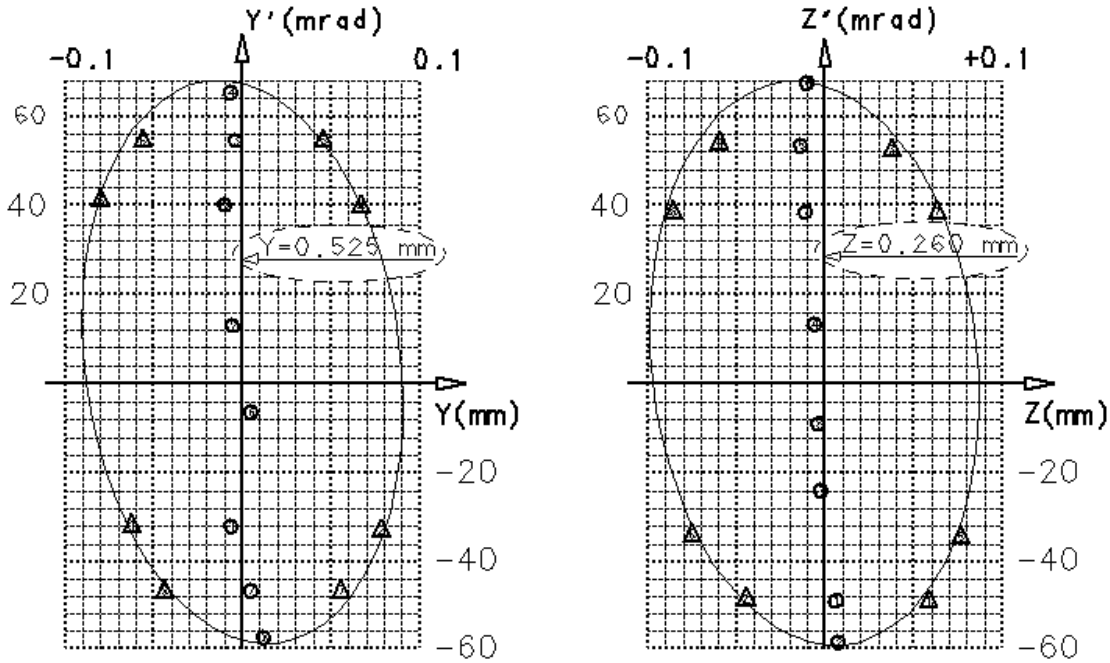

Fig. 7. Emittance diagram of the beam in the rear focal plane of the focusing lens; R_{max} = 8 mm, TILT = 5 mrad.

V. Bucking coil is shifted in the transverse plane

Finally, we need to understand the impact of some uncertainties in alignment of the coils in the lenses. As it was done earlier in [2], let's shift transversely one of the bucking coils. The beam will go along the axis of the main coil and the second bucking coil.

Fig. 8 shows emittance diagrams for 0.5 mm shift along Z.

Comparing the graphs with those in Fig. 3, we notice the shift of the beam centroid by ~0.19 mm in the Y direction and by ~0.19 mm in the Z direction. The beam centroid is also has a tilt of ~1 mrad towards the negative Y direction and the positive Z direction. Emittance of the beam found by calculation the area inside the representing ellipse is ~0.44 π mm-mrad. This emittance is quite similar to that of the ideal lens (0.42 π mm-mrad in Fig. 3). Similar exercise was made for a 1 mm shift of the front end bucking. Corresponding emittance diagram is shown in Fig. 9. The shift of the beam centroid for this case is ~0.38 mm in the Y direction and by ~0.4 mm in the Z direction. The beam centroid is also tilted by ~2 mrad towards the negative Y direction and by similar amount towards the positive Z direction.

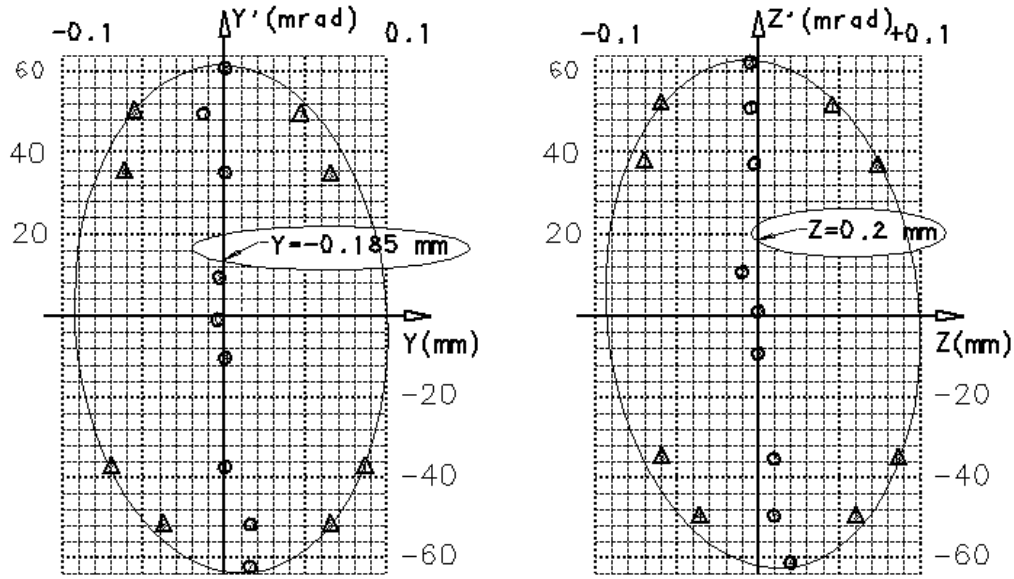

Fig. 8. Emittance diagram of the beam in the rear focal plane of the focusing lens; R_{max} = 8 mm; front end bucking coil is shifted 0.5 mm along Z-axis.

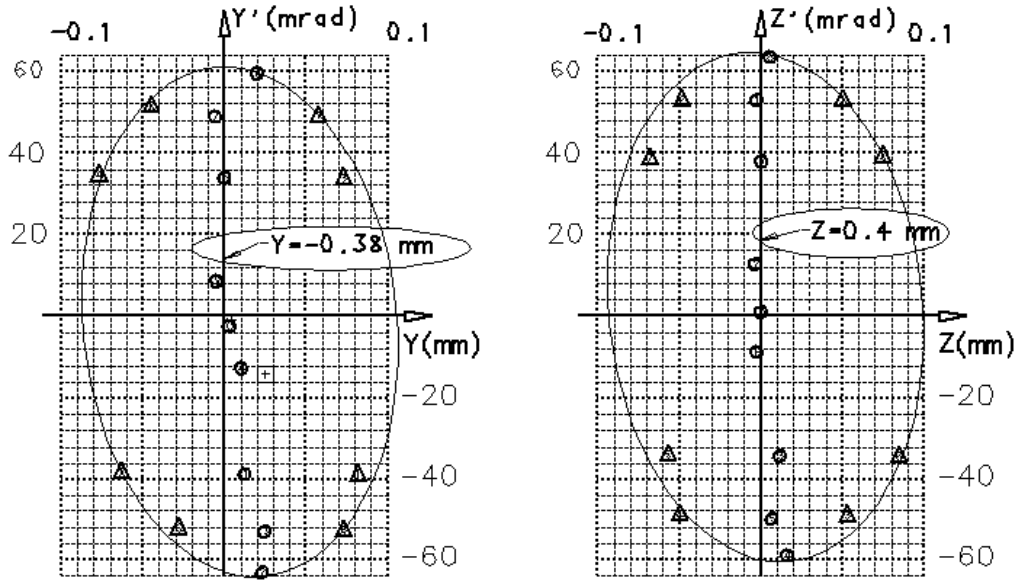

Fig. 9. Emittance diagram of the beam in the rear focal plane of the focusing lens; R_{max} = 8 mm; front end bucking coil is shifted 1.0 mm along Z-axis.

The deflection of the beam after the lens is proportional to the shift of the BC coil; as the expected maximum shift of the bucking coil from its nominal position is ~0.25 mm, we can conclude that the tilt of the beam centroid will not exceed ~0.7 mrad, which can result in the displacement at the next lens of ~0.5 mm.

Comparing the diagrams in Fig. 8 and Fig. 9 with that in Fig. 3, we can conclude that no significant emittance growth occurs as a result of the shift of the bucking coil.

VI. Scaling the Results and Lens Spacing Considerations

Integrated strength of the lens in combination with the beam energy chosen for this exercise will, most probably, never be used in the transport channel of the linac. The most recent design [4] uses focusing length that is approximately constant along the beam line, so the magnetic field in the lenses increases as a square root of the beam energy. Scaling of the results to this case can be made like the following:

1. For the same integrated strength of the lens and higher energy, the focusing length will change proportional to the energy (in accordance with the expression for the focusing lens in the Introduction). The length of the crossover region, that spans focal distances of sample traces with different radial position, will also change proportionally to the energy. The angles of the traces will be in the reversed proportion with the energy. This means that the transverse size of the crossover will remain the same, but angular size will be reduced, so the emittance growth will be in the reversed proportion to the energy. This conclusion is in a qualitative agreement with what was found in [1].
2. For the same beam energy and lower integrated strength of the lens, we also have increased focusing length (in the reversed proportion to the strength). So, the conclusions from the previous case remains.

Effectively, the analysis made in this note, was done for the worth case of the higher lens strength and lowest energy. In all possible cases, the situation must be better than it is found in this note. As a result, we can state with some degree of confidence that the maximum beam radius can be as large as 8 mm (or maybe even more) without resulting in the beam emittance increase due to the aberrations.

Important question is what spacing between the lenses can be accepted. Naturally, an answer depends on what radial size of the beam can be allowed. Simple analysis involving optical equivalent of the lenses shows that the phase advance on one periodicity element in terms of the Courant-Snider parameters can be defined using the next expression:

$$\cos(\mu) = 1 - L/2f$$

where L is the distance between lenses. Condition of stability in the Hill equation solution requires $0 < \mu < \pi$, so the distance L cannot be longer than 4f. On the other hand, beam pulsation factor $k = \sqrt{\beta_{max}/\beta_{min}}$ can be expressed as:

$$k = 1 / \sqrt{(1 - L/4)}$$

The choice of $L = 3 \cdot f$, results in $k=2$, which seems OK. With this assumption, $\beta_{max} \approx 2\sqrt{3} \cdot f$, and maximum beam radius

$$R_{max} = \sqrt{2\sqrt{3} f \cdot \varepsilon}$$

Let's assume that Rmax = 8 mm is a 5σ beam radius. Let's also take the value of the beam emittance as 25 times the desired normalized RMS emittance of 0.25 π mm-mrad: corresponding geometric emittance is then $\varepsilon_{5\sigma}=0.25\cdot10^{-3}\cdot25/0.073=86\cdot10^{-3}$ mm. Then we can find the required focal distance: $f_{5\sigma}$ = 215 mm and the distance between the lenses must be

~644 mm, which is in agreement with what was found in [4]. If Rmax = 8 mm is a 3σ beam radius, $\varepsilon_{3\sigma}$=0.25·10^{-3}·9/0.073 = 31·10^{-3} mm. In this case, the required focal distance becomes $f_{3\sigma}$ = 590 mm, and the distance between the lenses can be made ~1770 mm.

So, if to take into account relatively small expected emittance growth due to spherical aberrations in the lenses, we can try to increase the distance between the lenses to simplify mechanical requirements for the cryomodule design.

Beam losses must be carefully calculated in any case to ensure the loss does not exceed the allowed level of ~1 W/m.

VII. Conclusion

By using beam tracking option embedded in COMSOL electromagnetic module, we could analyze impact of some uncertainties in fabrication and positioning of the SS0 lens on the beam centroid position and beam emittance. Eight millimeter radius of the sample beam was accepted for this exercise to check limits of the lens. The energy of the particles (protons) in the beam was 2.5 MeV (β=0.0729).

With the initial normalized emittance of 0.4 π mm-mrad, the beam emittance is most sensitive to parallel displacement of the lens. The rate of the emittance growth is ~0.1 π mm-mrad per 1 mm of the shift. If 10% emittance growth can be accepted, the allowed parallel shift (or allowed deviation of the beam centroid from the center axis of the lens) is ~0.4 mm.

At the exit of the lens, the shift translates in the beam directed at the angle to the axis, with the angle defined by the focusing length. With 0.4 mm shift, this angle is 0.4/128 = 3.2 mrad; in turn, at the position of the next lens (625 mm), this angle will bring the beam centroid 2 mm off the axis, which is not acceptable. So, correction of the beam angle must be made to avoid this displacement. The corrector strength can be calculated based on the known angle:
BL = $\varphi \cdot \beta c \cdot m/e$. For φ = 3.2 mrad, required BL ≈ 0.07 T-cm.

Tilt of the lens, even if it is relatively large, although setting the beam off the axis, does not deteriorate emittance. E.g. 5 mrad tilt results in ~0.6 mm beam deflection from the axis in the focal plane and the angle of the beam centroid relative to the axis of ~5.6 mrad. Required total correction angle is ~7 mrad, which translates in the corrector strength BL ≈ 0.16 T-cm.

Even a very large (one millimeter) shift of the front end bucking coil of the lens results in ~0.55 mm beam deviation from the axis in the focal plane and ~3 mrad angle. To correct this, the required strength of the corrector must be BL ≈ 0.1 T-cm.

The three uncertainty factors working together (but in a statistically independent manner) result in the requirement of having corrector strength of ~0.2 T-cm. The requirement established by P. Ostroumov back in 2006 for the CH-type lens of the HINS linac front end was 0.25 T-cm (see also [5]), that seems quite reasonable. Dipole correctors introduced later in the SS1-type lens can provide much stronger deflecting pulse.

The study was made for the worst case of minimum energy and maximum length strength. In the environment of a beam transport system, beam emittance increase and deflections will be smaller, but required corrector strength will remain on the same level.

There is an indication, based on some qualitative analysis, that longer focusing period can work for the beam transport. This analysis did not take into account space charge and focusing action of RF cavities though, and further studies are required to understand rightness of this statement.

Another, quite formal analysis of optical properties of solenoid-based focusing lenses was made recently by V. Lebedev [7]. His study used longitudinal distribution of magnetic field in the prototype lenses built and tested for the front end of HINS linac, analyzed dangers of spherical aberration, and came to the conclusion that optical properties of solenoid-based lenses are quite adequate for use in the front end of the PX accelerator.

References:

1. I. Terechkine, “Beam Emittance Growth due to Aberrations in Focusing Lenses”, TD-10-005.
2. J. DiMarco, et al, “Optical Properties of a CH-type Focusing Lens”, TD-10-004
3. M. Tartaglia, et al, “Summary of HINS Focusing Solenoid Production and Test”, MT-21, China, Oct. 2009.
4. N.Solyak, “Project-X CW Linac Lattice Design”, March 16, 2010, http://projectx-docdb.fnal.gov/cgi-bin/ShowDocument?docid=450
5. G. Chlachidze, et. al, “HINS_SS1_SOL_02d Fabrication Summary and Test Results”, TD-09-001, FNAL, March 2009.
6. P. Ostroumov, “Beam Physics, Linac Lattice”, http://projectx-docdb.fnal.gov/cgi-bin/ShowDocument?docid=108
7. V. Lebedev, “An Estimate of Orbit Correction for SSR0 Section of the Project X” http://projectx-docdb.fnal.gov/cgi-bin/ShowDocument?docid=600